

Fault Localization for Synchrophasor Data using Kernel Principal Component Analysis

Ruonan CHEN, Xiaoying SUN, Guohong LIU

Department of Communication Engineering, Jilin University, Changchun, Jilin, 130022, China
graceliu@jlu.edu.cn

Abstract—In this paper, based on Kernel Principal Component Analysis (KPCA) of Phasor Measurement Units (PMU) data, a nonlinear method is proposed for fault location in complex power systems. Resorting to the scaling factor, the derivative for a polynomial kernel is obtained. Then, the contribution of each variable to the T^2 statistic is derived to determine whether a bus is the fault component. Compared to the previous Principal Component Analysis (PCA) based methods, the novel version can combat the characteristic of strong nonlinearity, and provide the precise identification of fault location. Computer simulations are conducted to demonstrate the improved performance in recognizing the fault component and evaluating its propagation across the system based on the proposed method.

Index Terms—power systems, fault location, phasor measurement units, kernel, principal component analysis.

I. INTRODUCTION

According to the trend of global energy internet, renewable energy has been introduced and widely adopted with high efficiency and large quantities in the world [1]. System structures and operation modes of power systems are increasingly complex [2]. Meanwhile, with the rapid development of industrialization and growth of population, electric energy demand has rapidly increased to make the system reach to its limits, thereby the sensitivity to faults in power systems is required urgently [3-4]. The blackout in North East American on the 14th August 2003 where 63 GW of load was interrupted, 531 generators were removed, and about \$7 billion were lost, which indicates that low speed of abnormal data acquisition and failure of fault location technology are the main reasons to cause a large scope and long time blackout [5].

To cope with the above problems, many countries have put emphasis on the development of the Wide Area Monitoring System (WAMS) which consists of a network of PMUs including GPS-synchronized technology [6-9]. PMUs can offer all kinds of electrical information at the rate of 30 or 60 samples per second. These intelligent systems make wide-area online monitoring of the operational status of power systems possible and have potential to greatly enhance wide-area visibility [10]. While PMUs offer massive data to describe operational status, how to reduce dimension and extract useful information efficiently becomes a major challenge.

Multivariate statistical techniques with the ability of dimension reduction are introduced in power systems to

estimate fault location [11-13], detect islanding [14] and event at an early stage [15], and identify system coherence [16]. In 2013, Barocio proposed a multivariate statistical projection method based on PCA with both the T^2 statistic and the Q statistic to estimate security operating margin and detect system disturbances [13]. However, the parameter causing fault can't be identified precisely which is one of the problems by PCA-based fault localization [17].

Consider nonlinearity arising in complex power systems, nonlinear methods should be proposed [15]. In 2016, with the large online synchrophasor data, Liu proposed an adaptive nonlinear approach which was applied to detect islanding [14]. Unfortunately, it can't provide the useful information of fault location for operators to prevent overspreading of event. In this paper, considering the fundamental nonlinearity arising in power systems, we firstly derive the expression of the derivative of polynomial kernel. Then the contribution of each PMU to T^2 statistic is defined. Finally, a novel nonlinear method is proposed for fault location in power systems one compared PCA method which can recognize fault component and evaluate its propagation across the system without knowledge of the system model/topology.

The rest of the paper is organized as follows: Section 2 introduces the principles of kernel principal component. Section 3 proposes a novel fault location algorithm with PMU data in complex power systems based on the KPCA model. In section 4, the simulated voltage event case demonstrates the effectiveness of proposed algorithm. Section 5 presents the conclusion of the whole paper.

II. BASIC KERNEL PRINCIPAL COMPONENT ANALYSIS (KPCA) ALGORITHM

In this paper, using KPCA maps PMU data from original space to feature space, we can extract the main information with minimum loss of nonlinear data.

Given a set of centered PMUs data $\mathbf{Y} \in R^{P \times N}$, wherein P presents the number of PMUs and N are samples:

$$\mathbf{Y} = (\mathbf{y}_1, \dots, \mathbf{y}_N) = \begin{bmatrix} y_{11} & y_{12} & \cdots & y_{1N} \\ y_{21} & y_{22} & \cdots & y_{2N} \\ \vdots & \vdots & \ddots & \vdots \\ y_{P1} & y_{P2} & \cdots & y_{PN} \end{bmatrix} \quad (1)$$

KPCA maps the observations into feature space with a possibly nonlinear map $\varphi: \mathbf{y} \in R^P \rightarrow \mathbf{z} \in R^F$. One can get the covariance matrix,

This work was supported in part by the by the National Nature Science Foundation of China (Grant 61171137), the '863' Research Project of China (Grant 625010217). The corresponding author: Guohong Liu.

$$\mathbf{S} = \frac{1}{N} \sum_{i=1}^N (\varphi(\mathbf{y}_i) - E\varphi(\mathbf{Y})) \sum_{i=1}^N (\varphi(\mathbf{y}_i) - E\varphi(\mathbf{Y}))^T \quad (2)$$

where $E\varphi(\mathbf{Y}) = \frac{1}{N} \sum_{i=1}^N \varphi(\mathbf{y}_i)$ represents the sample mean and T denotes transpose.

The eigenvalues and eigenvectors of \mathbf{S} are calculated as follows:

$$\begin{aligned} \lambda \mathbf{V} &= \mathbf{S} \mathbf{V} \\ &= \frac{1}{N} \sum_{i=1}^N \bar{\varphi}(\mathbf{y}_i) \bar{\varphi}(\mathbf{y}_i)^T \mathbf{V} \\ &= \frac{1}{N} \sum_{i=1}^N (\bar{\varphi}(\mathbf{y}_i)^T \mathbf{V}) \bar{\varphi}(\mathbf{y}_i) \end{aligned} \quad (3)$$

In (3), all eigenvectors \mathbf{V} corresponding eigenvalues are orthogonal and $\bar{\varphi}(\mathbf{y}_i) = \varphi(\mathbf{y}_i) - E\varphi(\mathbf{Y}), i = 1, \dots, N$.

Besides we can get a useful consequence by [18] that existing coefficients $\beta_i, i = 1, \dots, N$ can show the linear combination between the eigenvectors \mathbf{V} and the feature space data $\bar{\varphi}(\mathbf{y}_1), \dots, \bar{\varphi}(\mathbf{y}_N)$:

$$\mathbf{V} = \sum_{j=1}^N \beta_j \bar{\varphi}(\mathbf{y}_j) \quad (4)$$

Combining (3) and (4),

$$\frac{1}{N} \sum_{i=1}^N \bar{\varphi}(\mathbf{y}_i) \bar{\varphi}(\mathbf{y}_i)^T \sum_{j=1}^N \beta_j \bar{\varphi}(\mathbf{y}_j) = \lambda \sum_{j=1}^N \beta_j \bar{\varphi}(\mathbf{y}_j) \quad (5)$$

and left multiplying $\bar{\varphi}(\mathbf{y}_n), n = 1, \dots, N$ to both sides of (5), we can get

$$\begin{aligned} \frac{1}{N} \sum_{j=1}^N \beta_j \sum_{i=1}^N \langle \bar{\varphi}(\mathbf{y}_j) \cdot \bar{\varphi}(\mathbf{y}_i) \rangle \langle \bar{\varphi}(\mathbf{y}_n) \cdot \bar{\varphi}(\mathbf{y}_i) \rangle \\ = \lambda \sum_{j=1}^N \beta_j \langle \bar{\varphi}(\mathbf{y}_n) \cdot \bar{\varphi}(\mathbf{y}_j) \rangle \end{aligned} \quad (6)$$

where $\langle \cdot \rangle$ is the inner-product.

Actually, the F can be infinite so that it is infeasible to compute $\bar{\varphi}(\mathbf{y}_i)$ directly. We can define a kernel function k that just depends on the inner-product of feature space data [19],

$$k(\mathbf{y}_i, \mathbf{y}_j) = \langle \varphi(\mathbf{y}_i) \cdot \varphi(\mathbf{y}_j) \rangle \quad (7)$$

where k used in this paper is polynomial kernel,

$$k(\mathbf{y}_i, \mathbf{y}_j) = (\langle \mathbf{y}_i \cdot \mathbf{y}_j \rangle + c)^d \quad (8)$$

in which d is the order of polynomial, and $c = 0$ or $c = 1$ respectively represents homogeneous kernels and nonhomogeneous kernels.

The centered kernel matrix $\bar{\mathbf{K}}$ can be computed as follows:

$$\bar{\mathbf{K}} = \mathbf{K} - \mathbf{K} \mathbf{1} \mathbf{n} - \mathbf{1} \mathbf{n} \mathbf{K} + \mathbf{1} \mathbf{K} \mathbf{1} \mathbf{n} \quad (9)$$

where $\mathbf{K} = (\varphi(\mathbf{y}_1), \dots, \varphi(\mathbf{y}_N)) (\varphi(\mathbf{y}_1), \dots, \varphi(\mathbf{y}_N))^T$

and $\mathbf{1} \mathbf{n}_{ij} = 1/N, i, j = 1, \dots, N$.

Substituting (9) into (6), we can obtain

$$\frac{1}{N} \bar{\mathbf{K}} \bar{\mathbf{K}} \boldsymbol{\beta}_i = \lambda_i \bar{\mathbf{K}} \boldsymbol{\beta}_i \Rightarrow \bar{\mathbf{K}} \boldsymbol{\beta}_i = N \lambda_i \boldsymbol{\beta}_i, i = 1, \dots, N \quad (10)$$

So the eigenvalue decomposition of covariance matrix \mathbf{S} is transformed into the eigenvalue decomposition of kernel matrix $\bar{\mathbf{K}}$. Subsequently, the eigenvectors $\boldsymbol{\beta}_1, \dots, \boldsymbol{\beta}_N$ can be normalized by the following equation, more details being given in [20]:

$$1 = N \lambda_i \|\boldsymbol{\beta}_i\|^2, i = 1, \dots, N \quad (11)$$

Furthermore, getting the PCs $\mathbf{t} = \{t_1, t_2, \dots, t_k\}$ of the \mathbf{Y} by

$$\begin{aligned} t_i &= \langle \mathbf{V}_i \cdot \bar{\varphi}(\mathbf{y}) \rangle = \sum_{j=1}^N \beta_{j,i} \bar{\varphi}(\mathbf{y})^T \bar{\varphi}(\mathbf{y}_j) \\ &= \sum_{j=1}^N \beta_{j,i} \langle \bar{\varphi}(\mathbf{y}_j) \cdot \bar{\varphi}(\mathbf{y}) \rangle, i = 1, \dots, k \end{aligned} \quad (12)$$

where k is the number of PCs obtained by cumulative percent variance. $\beta_{j,i}$ is defined as the j^{th} element of the i^{th} eigenvalue of $\bar{\mathbf{K}}$.

III. ON-LINE MONITORING IN POWER SYSTEMS BASED ON KERNEL PRINCIPAL COMPONENT ANALYSIS

In this section, we propose such an event localization algorithm with the following features: 1) it is a nonlinear analysis version; 2) it can provide the accurate localization information of the fault bus.

For the purpose of fault location, both the T^2 statistic and the Q statistic are firstly used to identify the normal or unusual operating situation under the PMUs synchrophasor data. Secondly, based on the derivative of a polynomial kernel, getting the contribution of each variable to the T^2 statistic, we can achieve an accurate localization result and evaluate dynamic behavior of fault.

A. Detection of System Disturbances

On the basis of the (1), (9), (11), (12), we use the test data $\mathbf{y}_{test} \in R^P$ to calculate T_{new}^2 and Q_{new} statistics at current by

$$T_{new}^2 = \mathbf{t}_{new} \Delta^{-1} \mathbf{t}_{new}^T \quad (13)$$

$$Q_{new} = \sum_{i=1}^d (\mathbf{t}_{new,i})^2 - \sum_{i=1}^k (\mathbf{t}_{new,i})^2 \quad (14)$$

where $\mathbf{t}_{new,i} = \langle \mathbf{V}_i \cdot \bar{\varphi}(\mathbf{y}_{test}) \rangle = \sum_{j=1}^N \beta_{j,i} \langle \bar{\varphi}(\mathbf{y}_j) \cdot \bar{\varphi}(\mathbf{y}_{test}) \rangle$

and $\Delta = \text{diag}(\lambda_1, \dots, \lambda_k)$. d is the number of nonzero eigenvalues. Subsequently, T_{new}^2 and Q_{new} are compared to the given threshold [18] when one of the statistics is above it to present occurring of event.

B. Estimation of Fault Localization based on Contributions Plots

1) Calculating the derivative of kernel function

Kernel used in this paper is a polynomial kernel. Similar

to [21], introducing a scaling factor \mathbf{v} to the kernel function:

$$\begin{aligned} k(\mathbf{y}_j, \mathbf{y}_{test}) &= k((\mathbf{v} \cdot \mathbf{y}_j), (\mathbf{v} \cdot \mathbf{y}_{test})) \\ &= (\langle (\mathbf{v} \cdot \mathbf{y}_j) \cdot (\mathbf{v} \cdot \mathbf{y}_{test}) \rangle + c)^d \\ \mathbf{v} &= [v_1, \dots, v_p] = [1, \dots, 1] \\ j &= 1, \dots, N \end{aligned} \quad (15)$$

where (\bullet) is the componentwise vector product.

Consequently, one obtains the following derivative for a polynomial kernel by

$$\begin{aligned} \frac{\partial k(\mathbf{y}_j, \mathbf{y}_{test})}{\partial v_i} &= d \times (\langle (\mathbf{v} \cdot \mathbf{y}_j) \cdot (\mathbf{v} \cdot \mathbf{y}_{test}) \rangle + c)^{d-1} \\ &\quad \times 2 \times v_i \times y_{j,i} \times y_{test,i} \\ &= d \times (\langle \mathbf{y}_j \cdot \mathbf{y}_{test} \rangle + c)^{d-1} \\ &\quad \times 2 \times y_{j,i} \times y_{test,i} \Big|_{v_i=1} \end{aligned} \quad (16)$$

2) Obtaining the contribution of the T_{new}^2 statistic

The partial derivative of a function for a particular variable can represent the importance of the corresponding variable for the function [22]. Using the individual contribution defined in [23], we can estimate the influence of each PMU to T_{new}^2 statistic denoted as follows:

$$\begin{aligned} C_{T_{new,i}^2} &= \left| \frac{\partial T_{new}^2}{\partial v_i} \right| = \left| \frac{\partial}{\partial v_i} (\mathbf{t}_{new} \Delta^{-1} \mathbf{t}_{new}^T) \right| \\ &= \left| \frac{\partial}{\partial v_i} (\bar{\mathbf{K}}_{test} \boldsymbol{\mu} \Delta^{-1} \boldsymbol{\mu}^T \bar{\mathbf{K}}_{test}^T) \right| \\ &= \left| \frac{\partial}{\partial v_i} (\text{trace}(\boldsymbol{\mu}^T \bar{\mathbf{K}}_{test}^T \bar{\mathbf{K}}_{test} \boldsymbol{\mu} \Delta^{-1})) \right| \\ &= \left| \text{trace}(\boldsymbol{\mu}^T (\frac{\partial}{\partial v_i} \bar{\mathbf{K}}_{test}^T \bar{\mathbf{K}}_{test}) \boldsymbol{\mu} \Delta^{-1}) \right| \end{aligned} \quad (17)$$

where $\boldsymbol{\mu} = (\boldsymbol{\beta}_1, \dots, \boldsymbol{\beta}_k)$.

We respectively calculate kernel matrix $\bar{\mathbf{K}}_{test}$ of the test data and the partial derivative $\frac{\partial \bar{\mathbf{K}}_{test}}{\partial v_i}$:

$$\bar{\mathbf{K}}_{test} = \mathbf{K}_{test} - \mathbf{L}\mathbf{K} - \mathbf{K}_{test} \mathbf{L}\mathbf{n} + \mathbf{L}\mathbf{K}\mathbf{L}\mathbf{n} \quad (18)$$

$$\frac{\partial \bar{\mathbf{K}}_{test}}{\partial v_i} = (\frac{\partial \bar{\mathbf{K}}_{test,1}}{\partial v_i}, \frac{\partial \bar{\mathbf{K}}_{test,2}}{\partial v_i}, \dots, \frac{\partial \bar{\mathbf{K}}_{test,N}}{\partial v_i}) \quad (19)$$

where $\mathbf{L} = 1/N[1, \dots, 1] \in R^{1 \times N}$.

According to (17), (18), and (19), it is simple that the partial derivative of the j^{th} element of $\bar{\mathbf{K}}_{test}$ to v_i is offered by (20). Because the second and the fourth elements of $\bar{\mathbf{K}}_{test,j}$ have nothing to do with \mathbf{y}_{test} , we regard them as constant values. Furthermore, the simple version of

$\frac{\partial \bar{\mathbf{K}}_{test,j}}{\partial v_i}$ can be derived as follows:

$$\begin{aligned} \frac{\partial \bar{\mathbf{K}}_{test,j}}{\partial v_i} &= \frac{\partial}{\partial v_i} (k(\mathbf{y}_j, \mathbf{y}_{test}) - \frac{1}{N} \sum_{n=1}^N k(\mathbf{y}_j, \mathbf{y}_n) \\ &\quad - \frac{1}{N} \sum_{n=1}^N k(\mathbf{y}_n, \mathbf{y}_{test}) + \frac{1}{N^2} \sum_{m=1}^N \sum_{n=1}^N k(\mathbf{y}_m, \mathbf{y}_n)) \\ &= \frac{\partial}{\partial v_i} (k(\mathbf{y}_j, \mathbf{y}_{test}) - \frac{1}{N} \sum_{n=1}^N k(\mathbf{y}_n, \mathbf{y}_{test})) \\ &= 2d (\langle \mathbf{y}_j \cdot \mathbf{y}_{test} \rangle + c)^{d-1} y_{j,i} y_{test,i} \\ &\quad - \frac{2}{N} \sum_{n=1}^N d (\langle \mathbf{y}_n \cdot \mathbf{y}_{test} \rangle + c)^{d-1} y_{n,i} y_{test,i} \Big|_{v_i=1} \end{aligned} \quad (20)$$

Besides, it is essential to derive the partial derivative of $\frac{\partial (\bar{\mathbf{K}}_{test}^T \bar{\mathbf{K}}_{test})_{nm}}{\partial v_i}$, where $(\bar{\mathbf{K}}_{test}^T \bar{\mathbf{K}}_{test})_{nm}$ is defined as the

element of the n^{th} row and the m^{th} column of $\bar{\mathbf{K}}_{test}^T \bar{\mathbf{K}}_{test}$.

Using the expression (20), the specific expression can be got

$$\begin{aligned} \frac{\partial (\bar{\mathbf{K}}_{test}^T \bar{\mathbf{K}}_{test})_{nm}}{\partial v_i} &= \frac{\partial \bar{\mathbf{K}}_{test,n}}{\partial v_i} \bar{\mathbf{K}}_{test,m} + \bar{\mathbf{K}}_{test,n} \frac{\partial \bar{\mathbf{K}}_{test,m}}{\partial v_i} \\ &= (2d (\langle \mathbf{y}_n \cdot \mathbf{y}_{test} \rangle + c)^{d-1} y_{n,i} y_{test,i} \\ &\quad - \frac{2}{N} \sum_{j=1}^N d (\langle \mathbf{y}_j \cdot \mathbf{y}_{test} \rangle + c)^{d-1} y_{j,i} y_{test,i} \Big|_{v_i=1}) \bar{\mathbf{K}}_{test,m} \\ &\quad + (2d (\langle \mathbf{y}_m \cdot \mathbf{y}_{test} \rangle + c)^{d-1} y_{m,i} y_{test,i} \\ &\quad - \frac{2}{N} \sum_{j=1}^N d (\langle \mathbf{y}_j \cdot \mathbf{y}_{test} \rangle + c)^{d-1} y_{j,i} y_{test,i} \Big|_{v_i=1}) \bar{\mathbf{K}}_{test,n} \end{aligned} \quad (21)$$

Substituting (21) into (17), the contribution $C_{T_{new,i}^2}$ of the i^{th} PMU to T_{new}^2 statistic is obtained. If a PMU has a maximum value of contribution $C_{T_{new,i}^2}$, the corresponding bus is the source of event. The proposed algorithm for fault localization is summarized in Table I.

TABLE I. THE STEP OF FAULT LOCALIZATION ALGORITHM BASED ON KERNEL PRINCIPAL COMPONENT ANALYSIS

Once the fault is detected, the proposed algorithm is executed.
1: Use (16) to calculate the derivative for a polynomial kernel;
2: According to the derivative, the training matrix \mathbf{Y} , the test vector \mathbf{y}_{test} , and (21), the each element of $\frac{\partial}{\partial v_i} \bar{\mathbf{K}}_{test}^T \bar{\mathbf{K}}_{test}$ can be got, where $i = 1, \dots, P$;
3: Substituting the leading eigenvalues $\Delta = \text{diag}(\lambda_1, \dots, \lambda_k)$, the corresponding eigenvectors $\boldsymbol{\beta}_1, \dots, \boldsymbol{\beta}_k$, and $\frac{\partial}{\partial v_i} \bar{\mathbf{K}}_{test}^T \bar{\mathbf{K}}_{test}$ into (17), we can successively obtain $C_{T_{new,1}^2}, \dots, C_{T_{new,p}^2}$;
4: Selecting the most value of $C_{T_{new,1}^2}, \dots, C_{T_{new,p}^2}$, the corresponding bus is the fault component.

IV. EVALUATION USING SIMULATED CASES

In this section, we use an illustrative example to identify the efficacy of fault location of the proposed algorithm, and compare its performance with the PCA based method in [13]. A 9-bus 3-generator system is used to generate

synchrophasor data shown in Fig. 1, where a PMU is placed at each bus and the sampling rate is 50Hz. The significance level of two statistics T^2 and Q is set to 0.01. In order to mimic the industry-grade PMUs, noise is added to this simulated data so that the signal-to-noise(SNR) is 92dB [15].

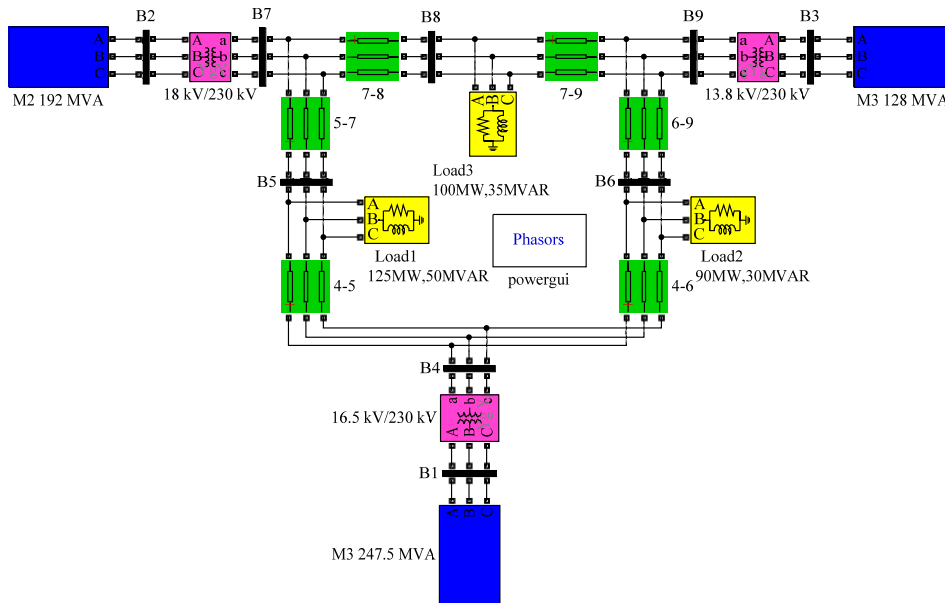


Figure 1. Electric diagram of IEEE 9-bus system

As Fig. 2 displays, a single-phase to ground fault is applied at bus 6 cleared in 200ms by opening the line between buses 6 and 4. We assume the training matrix is $Y \in R^{9 \times 1000}$ collected from normal operating conditions and the simulated time changes from 120s to 160s.

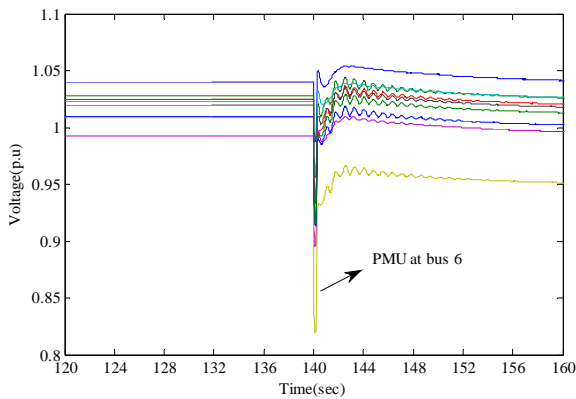


Figure 2. Voltage variation indicating a single-phase to ground fault

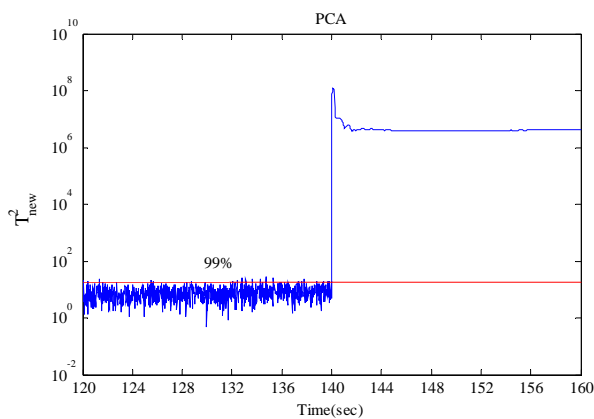


Figure 3. The T^2 statistic for detection of the single-phase to ground fault based on the PCA model in [13]

Fig. 3 and Fig. 4 show both the T^2_{new} statistic and the Q_{new} statistic for detection of single-phase to ground fault based on the PCA model in [13]. Fig. 5 and Fig. 6 show both the T^2_{new} statistic and the Q_{new} statistic for detection of single-phase to ground fault based on the KPCA model. It is clear that KPCA has fewer false alarms than PCA. Besides, two operating conditions can be identified that the first 20 seconds of the simulation are normal operating region and the last 20 seconds are the fault. However, the above two ways can fail to identify the new stable operating conditions after fault because the models and corresponding thresholds are not adaptive.

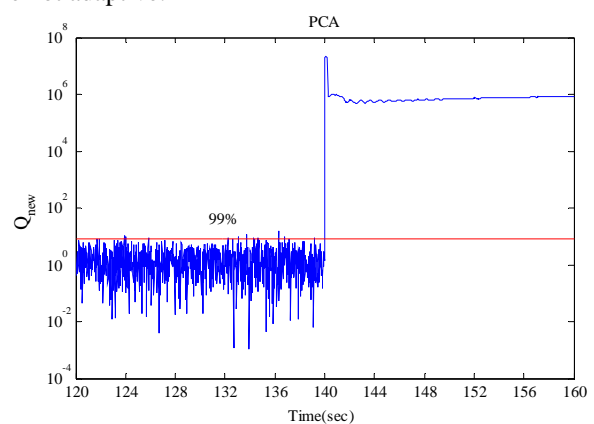


Figure 4. The Q statistic for detection of the single-phase to ground fault based on the PCA model in [13]

When a fault is occurring in the system, the proposed algorithm can be operated to estimate the source. Comparing the Fig. 7 with Fig. 8, it can be effectively proved that the proposed algorithm in this paper can offer more accurate result of fault location than [13].

Fig. 7 shows that the 6th, 9th buses are mainly responsible for event occurrence. As previously noted, the PCA

approach proposed by [13] can not obtain a precise result for fault parameter.

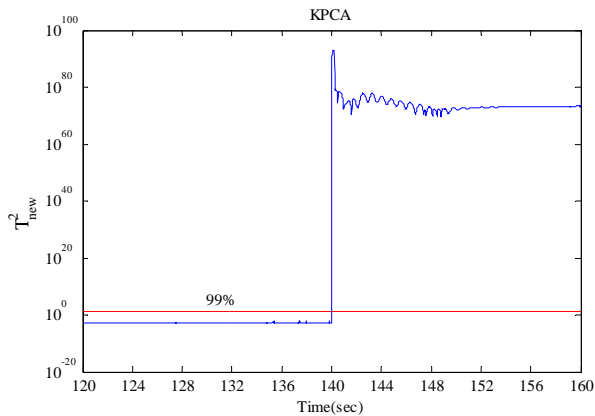


Figure 5. The T^2 statistic for detection of the single-phase to ground fault based on the KPCA model

Unlike Fig. 7, Fig. 8 shows the 6th bus is mainly responsible for event occurrence and it is the biggest one to represent the event source. As previously noted, the proposed algorithm can exact veracious achieve the goal of event location. Furthermore, the results of two algorithms are summarized clearly in Table II.

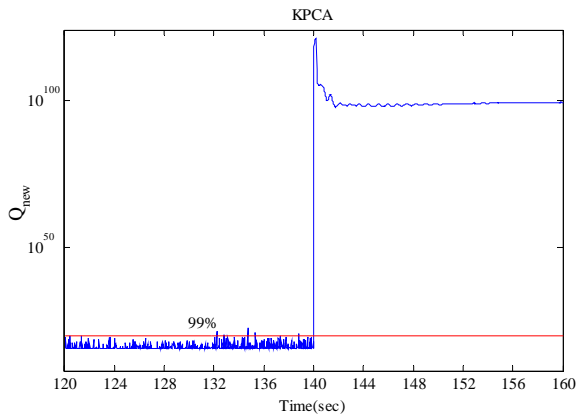


Figure 6. The Q statistic for detection of the single-phase to ground fault based on the KPCA model

To improve the visualization of event evolution, Fig. 9 shows the contribution map during the first 20 seconds after the fault is cleared. It shows that buses 3, 6, 8, 9, present the

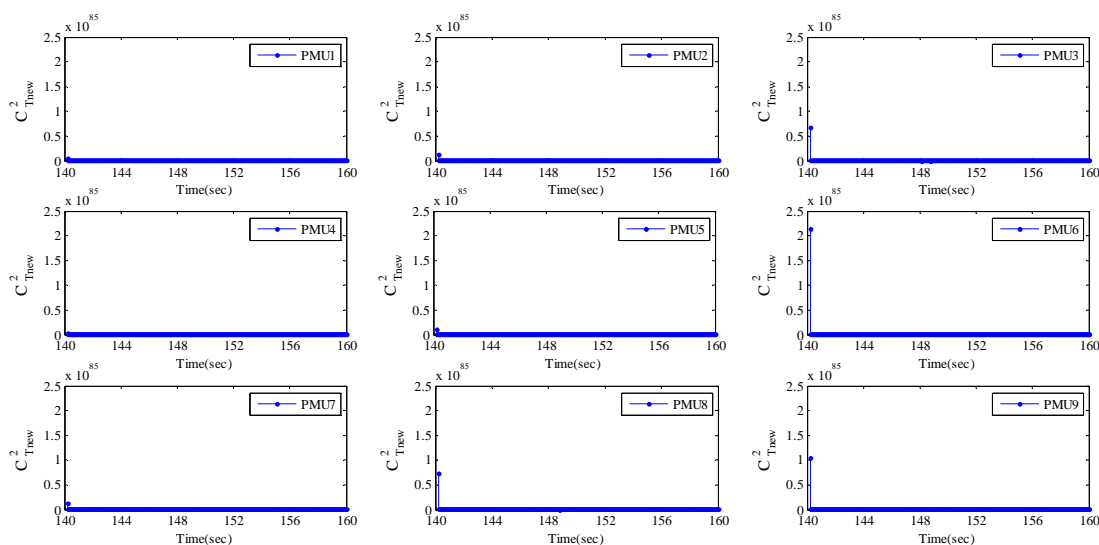


Figure 9. Contribution map visualization to T^2 statistic for location of the single-phase to ground fault based on the KPCA model

highest contributions, followed by PMUs located at buses 1, 2, 4, 5, 7. The results suggest intense dynamic participation of the generators from different areas of the system and confirm that the fault is spreading across the system.

TABLE II. THE SUMMARY OF LOCATION RESULT

	simulate condition	PCA	KPCA
fault range	bus6	bus6 bus9	bus6
fault location	bus6	bus6	bus6

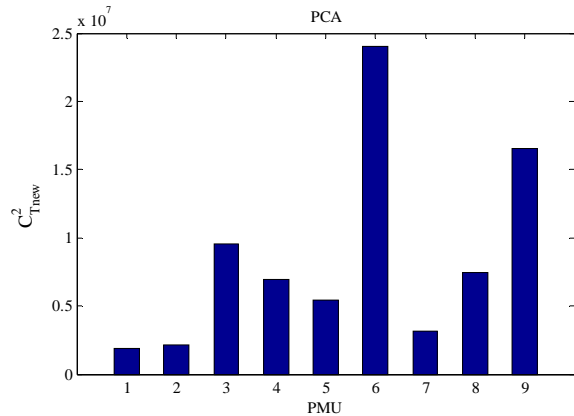


Figure 7. Contribution plot to the T^2 statistic for location of the single-phase to ground fault based on the PCA model at fault inception point

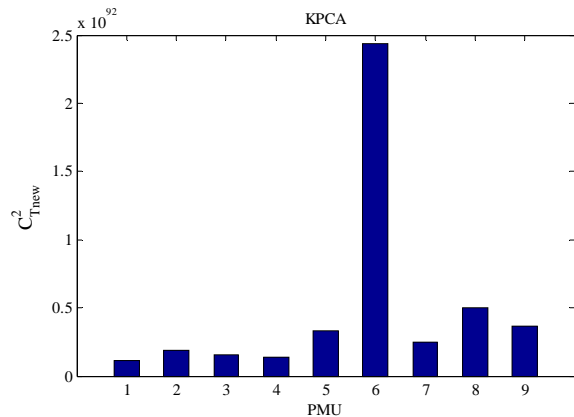


Figure 8. Contribution plot to the T^2 statistic for location of the single-phase to ground fault based on the KPCA model at fault inception point

V. CONCLUSIONS

In this paper, a nonlinear method for fault location in power systems is proposed. Based on KPCA, the nonlinear analysis of wide-area synchronized PMUs data is realized. According to the derived contribution of each variable to T^2 statistic under a polynomial kernel, the novel version can offer a good estimation about the fault location and propagation across the power systems. Comparative analysis between the proposed algorithm and PCA based methods reveal that the former has superior reliability to identify fault source and evaluate system behaviour.

In the future, the research includes the following aspects: 1) more robust algorithm will be developed to reveal the effect of characteristic of time-varying of power systems and detect equilibrium point adaptively to reduce the false alarm. 2) It is meaningful to use more realistic data to verify the performance of the proposed algorithm.

REFERENCES

- [1] X. Liu, D. M. Lavery, R. J. Best, K. Li, D. J. Morrow, S. McLoone, "Principal component analysis of wide-area phasor measurements for islanding detection - a geometric view," *IEEE Transactions on Power Delivery*, vol. 30, no. 2, pp. 976-985, 2015. doi: 10.1109/TPWRD.2014.2348557
- [2] W. J. Liu, Z. Z. Lin, F. S. Wen, G. Ledwich, "A wide area monitoring system based load restoration method," *IEEE Transactions on Power Systems*, vol. 28, no. 2, pp. 2025-2034, 2013. doi: 10.1109/TPWRS.2013.2249595
- [3] Z. Zhao, C. Wang, Y. G. Zhang, Y. Sun, "Latest progress of fault detection and localization in complex electrical engineering," *Journal of Electrical Engineering*, vol. 65, no. 1, pp. 55-59, 2014. doi: 10.2478/jee-2011-0008
- [4] D. Novosel, K. Vu, V. Centeno, S. Skok, M. Begovic, "Benefits of synchronized-measurement technology for power-grid applications", in Proc. 4th Annu. Hawaii Int. Conf. System Sciences, Hawaii, 2007, pp. 118-118. doi: 10.1109/hicss.2007.106
- [5] M. Rarrerty, X. Liu, D. Lavery, S. McLoone, "Real-time multiple event detection and classification using moving window pca," *IEEE Transactions on Smart Grid*, vol. 7, no. 5, pp. 2537-2548, 2015. doi: 10.1109/TSG.2016.2559444
- [6] S. Abraham, H. Dhaliwal, R. J. Efford, L. J. Keen, A. McLellan, J. Manley, K. Vollman, N. J. Diaz, T. Ridge et al., "Final report on the August 14, 2003 blackout in the United states and Canada: causes and recommendations. US-Canada Power System Outage Task Force, 2004
- [7] Y. Wang, W. Y. Li, J. P. Lu, "Reliability analysis of phasor measurement unit using hierarchical markov modeling," *Electric Power Components and Systems*, vol. 37, no. 5, pp. 517-532, 2009. doi: 10.1080/15325000802599361
- [8] R. Sodhi, S. C. Srivastava, S. N. Singh, "Phasor-assisted hybrid state estimator," *Electric Power Components and Systems*, vol. 38, no. 5, pp. 533-544, 2010. doi: 10.1080/15325000903376925
- [9] R. Sodhi, S. C. Srivastava, S. N. Singh, "Optimal pmu placement method for complete topological and numerical observability of power system," *Electric Power Components and Systems*, vol. 80, no. 9, pp. 1154-1159, 2010. doi: 10.1016/j.epr.2010.03.005
- [10] C. H. Peng, H. J. Sun and J. F. Guo, "Multi-objective optimal pmu placement using a non-dominated sorting differential evolution algorithm," *International Journal of Electrical Power & Energy Systems*, vol. 32, no. 8, pp. 886-892, 2010. doi: 10.1016/j.jipeps.2010.01.024
- [11] Arturo. R. Messina, N. I. Moreno, J. J. Nuno, "Monitoring the health of large interconnected power systems: a near real-time perspective," in Proc. 8th Annu. IFAC Symposium on Fault Detection, Supervision and Safety of Tehnical Processes(SAFEPROCESS), Mexico, 2012, pp. 2-12. doi: 10.3182/20120829-3-MX-2028.00301
- [12] Y. G. Zhang, Z. P. Wang, J. F. Zhang, "A novel fault identification using WAMS/PMU," *Advances in Electrical and Computer Engineering*, vol. 12, no. 2, pp. 21-26, 2012. doi: 10.4316/AECE.2012.02004
- [13] E. Barocio, B. C. Pal, D. Fabozzi, N. F. Thornhill, "Detection and visualization of power system disturbances using principal component analysis," in Proc. IREP, 2013, pp. 1-10. doi: 10.1109/IREP.2013.6629374
- [14] X. Liu, J. M. Kennedy, D. M. Lavery, D. John Morrow, Sean McLoone, "Wide area phase angle measurements for islanding detection – an adaptive nonlinear approach", *IEEE Transactions on Power Delivery*, vol. 31, no. 4, pp. 1901-1911, 2016. doi: 10.1109/TPWRD.2016.2518019
- [15] Le. Xie, Yang. Chen, P. R. Kumar, "Dimensionality reduction of synchrophasor data for early event detection: linearized analysis," *IEEE Transactions on Power System*, vol. 29, no. 6, pp.2784-2794, 2014. doi: 10.1109/TPWRS.2014.2316476
- [16] M. Ariff, B. C. Pal, "Coherency identification in interconnected power systems – an independent component analysis approach", *IEEE Transactions on Power System*, vol. 20, no. 2, pp. 1747-1755, 2013. doi: 10.1109/TPWRS.2012.2217511
- [17] Ali. Ajami, Mahdi. Daneshvar, "Data driven approach for fault detection and diagnosis of turbine in thermal power plant using independent component analysis," *Electrical Power and Energy Systems*, vol. 43, no. 1, pp.728-735, 2012. doi: 10.1016/j.jipeps.2012.06.022
- [18] Jong. Min. Lee, Chang. Kyoo, Yoo, Sang. Wook Choi, Peter. A. Vanrolleghem, In. Beum. Lee, "Nonlinear process monitoring using kernel principal component analysis", *Chemical Engineering Science*, vol. 59, no. 1, pp. 223-234, 2004. doi: 10.1016/j.ces.2003.09.012
- [19] Shujie. Hou, Robert. Caiming. Qiu, "Kernel feature template matching for spectrum sensing," *IEEE Transactions on Vehicular technology*, vol. 63, no. 5, pp. 2258-2271, 2014. doi: 10.1109/TVT.2013.2290866
- [20] Bernhard Schölkopf, Alexander Smola, Klaus-Robert Müller, "Nonlinear component analysis as a kernel eigenvalue problem," *Neural Computation*, vol. 10, no. 5, pp. 1299-1319, 1998. doi: 10.1162/089976698300017467
- [21] A. Rakotomamonjy, "Variable selection using svm based criteria," *Journal of Machine Learning Research*, vol. 3, no. 3, pp. 1357-1370, 2003
- [22] F. Jia, E. B. Martin, A. J. Morris, "Non-linear principal components analysis with application to process fault detection," *International Journal of Systems Science*, vol. 31, no. 11, pp. 1473-1487, 2001. doi: 10.1080/00207720050197848
- [23] J.-H. Hu, S.-S. Xie, G.-Q. Luo, F. Yang, J.-B. Peng, "Fault identification method of kernel principal component analysis based on contribution plots and its application," *Systems Engineering and Electronics*, vol. 30, no. 3, pp. 572-576, 2008